

A LES BASED SOUND ABSORPTION ANALYSIS OF HIGH-AMPLITUDE WAVES THROUGH AN ORIFICE WITH BIAS FLOW

A. Scarpato*, S. Ducruix, T. Schuller
École Centrale Paris, Laboratoire EM2C, CNRS
Grande Voie des Vignes
Châtenay-Malabry - 92295
Email: alessandro.scarpato@em2c.ecp.fr

ABSTRACT

Thermo-acoustic instabilities and, more generally, the noise associated with combustion dynamics in high-performance combustion systems are of increasing concern to gas turbine manufacturers. One way to hinder these phenomena is to improve acoustic damping. A perforated plate with a bias flow can be very efficient in fulfilling this function, as long as it is properly designed. This system operates by converting incident acoustic energy into kinetic energy of the flow field, which is then quickly dissipated by turbulence. However this mechanism is not entirely understood, especially at high amplitude pressure fluctuations. The present study deals with the different responses of an orifice traversed by a bias flow, in linear and nonlinear regimes, when subjected to incident sound waves. Large Eddy Simulation (LES) is used to analyze the flow field through the aperture, calculate its reflection and transmission coefficients and analyze sound absorption as a function of the perturbation level. It is shown that the velocity fluctuation level u'_0 within the perforation plays a key role in the dissipation process. A transition occurs when u'_0 exceeds the mean bias flow velocity within the orifice $u'_0 > \bar{u}_0$ and reverse flow is observed, leading to major changes in the balance between reflection and transmission processes. It is however shown that absorption remains approximately independent of the sound level even at the high amplitudes simulated in the present paper up to $u'_0/\bar{u}_0 \sim 10$. The evolution with the perturbation level of the unsteady pressure loss through the perforation is then examined using different analytical models. Predictions are compared with simulation results. Differences are observed

in the transition between the linear and nonlinear regimes.

INTRODUCTION

Gas turbine manufacturers are greatly concerned with the problems arising from the interaction between acoustics and combustion dynamics [1, 2]. Perforated screens backed by a resonant cavity are widely used for acoustic damping in industrial applications. In a recent study [3], perforated screens designed using available linear models [4, 5] and placed at the rear side of a premixing system were used to hinder longitudinal thermo-acoustic instabilities in a turbulent swirled burner. The damper was shown to operate well for small pressure disturbances in the frequency range 250 to 400 Hz and the results were consistent with the model predictions. It eventually fails when the instability oscillation level raises inside the chamber [6]. The objective of the present study is to analyze the transition between linear and nonlinear regimes in the sound absorption process to design robust damping systems at high sound pressure levels.

Due to the wide variety of applications, extensive research has been devoted to the experimental characterization, modeling and simulation of the absorption properties of perforated screens. Effects of the plate porosity, thickness, geometry of the apertures or of the inner structure, ducting of the apertures or interactions between the holes were thoroughly examined (see for example [7, 8, 9, 10, 11, 12, 13]). We restrict here the analysis to thin perforates traversed by a bias flow and subjected to normal sound waves of increasing amplitudes. Recently, Rupp *et al.* [14] carried out an experimental study on the effect of excitation am-

*Address all correspondence to this author.

plitude on the absorption of a single orifice with a mean bias flow. The transition between the linear and nonlinear regimes is studied using PIV measurements and it is shown that absorption reaches a maximum when the sound level is increased before being attenuated at higher levels. This type of response was already noted in the experiments gathered by Ingard and Ising [15]. A few numerical studies have already been conducted on the absorption properties of perforated plates with a bias flow. Leung *et al.* [16] studied the effects of frequency and orifice opening size on absorption by direct simulations in two dimensions. They found that absorption is improved at low forcing frequencies and for small orifices. Large Eddy Simulation (LES) was also used by Mendez *et al.* [17] to study the response of perforates, restraining their study to the linear regime. Analytical expressions were proposed by different authors [15, 18, 19, 20] to determine the impedance of perforated plates operating in linear and nonlinear regimes. These models include different lumped parameters whose values must be determined. It is thus worth examining the flow dynamics in the vicinity of the orifice to get insight in the mechanisms responsible for acoustic dissipation using detailed experiments or simulations.

This study aims at understanding the change in the response of a perforated plate from linear to nonlinear regime, when it is subjected to incident acoustic waves of increasing amplitude at a given forcing frequency. Three-dimensional LES is used to simulate the flow through an orifice at isothermal ambient conditions, allowing a detailed analysis of the flow dynamics near the orifice. In the simulations carried out here, a single circular aperture is placed in a square-section domain, with a uniform steady flow. The inlet acoustic boundary condition is non-reflecting, and the outlet is pulsed with harmonic modulations. The forcing frequency is chosen to obtain conditions close to optimal absorption of the incident sound waves at low amplitudes.

The classical model developed by Howe [4] describing the sound absorption of perforates in the linear regime is presented in the next section. Predictions with this model are then compared to numerical results, which are shown to be in good agreement for small modulation levels, validating the methodology. The aperture is then subjected to increasing sound levels, ranging from 90 up to 150 dB. In this way both the linear and nonlinear responses of the damper can be investigated. The transition between these two regimes is then studied and is shown to depend on the resulting velocity perturbation level within the orifice. It is in particular shown that absorption properties remain approximately constant at high amplitudes, but the region within the flow where acoustic incident energy is dissipated changes between the linear and nonlinear regimes.

ACOUSTIC ANALYSIS

We consider the case of a thin perforated plate with a steady bias flow through the orifices, subjected to normal incident pres-

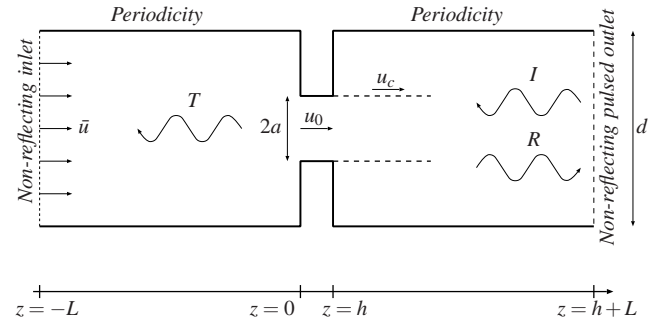


FIGURE 1: SCHEMATIC VIEW OF THE COMPUTATIONAL DOMAIN. FLOW FROM LEFT TO RIGHT. ACOUSTIC MODULATION IS IMPOSED ON THE RIGHT BOUNDARY CONDITION.

sure waves. The central issue is to determine the Rayleigh conductivity linking the fluctuating volume flowrate within the perforations and acting as a sound source to the unsteady pressure difference applied to the plate. Assuming harmonic fluctuations, the fluctuating pressure p' and velocity u' write:

$$p' = \text{Re} \{ \tilde{p} \exp(-i\omega t) \}, \quad u' = \text{Re} \{ \tilde{u} \exp(-i\omega t) \} \quad (1)$$

where $\omega = 2\pi f$ is the angular frequency. Using these notations, the Rayleigh conductivity of the aperture is defined as:

$$K_R = -\frac{i\omega\rho\tilde{q}}{\Delta\tilde{p}} \quad (2)$$

where ρ is the mean fluid density, $q' = \text{Re} \{ \tilde{q} \exp(-i\omega t) \}$ is the fluctuating volume flowrate and $\Delta\tilde{p} = [\tilde{p}_u - \tilde{p}_d]$ is the fluctuating pressure difference applied to the plate. The Rayleigh conductivity is a function of the geometry of the aperture, the bias flow velocity, the frequency and the sound level [15, 18]. For small perturbations it is possible to derive an analytical expression for this quantity.

Howe's model

The Reynolds number within the perforation is usually large enough ($\text{Re} \gg 1$) to neglect viscous effects except near the edges where flow separation takes place. This type of behaviour has been modelled by Howe [4] for a circular aperture of radius a in which a steady jet emerges irrotationally, separated from the ambient medium by an infinitely thin vortex sheet (Fig. 1). Vortices created at the aperture edges are swept away by the flow with a velocity u_c . The following analytical expression for a cylindrical vortex sheet of radius a and a constant vortex convection velocity

u_c can be obtained [4]:

$$K_R = 2a(\gamma - i\delta) \quad (3)$$

The coefficients γ and δ are positive functions of the Strouhal number $St = \omega a / u_c$:

$$\gamma - i\delta = 1 + \frac{\pi/2I_1(St)\exp(-St) - iK_1(St)\sinh(St)}{St[\pi/2I_1(St)\exp(-St) + iK_1(St)\cosh(St)]} \quad (4)$$

where I_1 and K_1 are modified Bessel functions of the first and second kinds. Note that the vortex convection velocity u_c is often taken equal to the bias flow velocity ($u_c = u_0$) within the perforation without clear justification [5]. Howe mentioned that this velocity equals half that of the jet velocity $u_c = u_j/2$ [4]. This however does not take into account the *vena contracta* effect [21]. Many models were derived based on the original expression Eq. (4), including plate thickness [10, 22], hole shape [23] or ducting effects [9]. These models are however limited to small pressure perturbations and alternative approaches were proposed to take into account the effects of sound level [15, 18].

It is generally easier to examine the reflection and transmission coefficients far from the perforate instead of the Rayleigh conductivity which requires the knowledge of the pressure difference across the plate and the velocity within the perforation.

Reflection, transmission and absorption

Assuming plane waves propagation away from the orifice, one can relate the reflection, transmission and absorption coefficients to the Rayleigh conductivity. Small orifices, compact with respect to the flow disturbances considered, can be characterized by two jump conditions. The first one is given by the definition of K_R (Eq. 2). The second condition is given by the conservation of the acoustic volume flowrate q' through the aperture $\tilde{q} = \tilde{u}_d d^2 = \tilde{u}_u d^2$. In this expression \tilde{u}_d and \tilde{u}_u denote the acoustic velocity fluctuation downstream and upstream the perforation within the square domain of cross section d^2 (Fig. 1). By combining these jump conditions, the reflection coefficient R and the transmission coefficient T can be written as:

$$R = -\frac{ikd^2}{2K_R} \left(1 - \frac{ikd^2}{2K_R}\right)^{-1}, \quad T = \left(1 - \frac{ikd^2}{2K_R}\right)^{-1}, \quad (5)$$

where $k = \omega/c$ is the wave number, and c is the sound speed. Finally, the absorption coefficient is given by:

$$\alpha = 1 - |R|^2 - |T|^2 \quad (6)$$

It is worth noting that absorption is limited to $\alpha_{\max} = 0.5$ for a non reflecting duct at $z = -L$ (Fig. 1) [8].

NUMERICAL CONFIGURATION

Simulations in this study were conducted with the LES solver AVBP, developed at Cerfacs (www.cerfacs.fr/4-26334-The-AVBP-code.php).

It solves the compressible Navier-Stokes equations on unstructured meshes based on a Large Eddy Simulation framework, using explicit methods. The simulations in this paper are carried out with the finite-volume Lax-Wendroff scheme [24], which is second order accurate in space and time. The subgrid-scale stress model used to close the turbulent fluxes is based on the WALE model [25]. Inlet and outlet boundary conditions are treated with the Navier-Stokes Characteristic Boundary Conditions (NSCBC) method [26].

The configuration simulated in this paper aims at modeling the unsteady flow through a perforated plate with a regular distribution of holes. Since the number of apertures can be important, it is out of reach to try to simulate the whole plate. Thus only a single hole is considered here, and periodic conditions are used at the lateral boundaries of the numerical domain to take into account the presence of an array of apertures distributed over a square mesh. The symmetry of the problem is fixed by these conditions and asymmetrical interactions between the orifices are not considered here. Asymmetry would for example be triggered by an instability in the flow within the perforation but this probably only takes place at very high sound levels. The orifice walls are modeled with a no-slip condition.

Figure 1 shows a schematic view of the numerical domain. The domain has a square section with $d = 6$ mm. This distance also represents the separation between two apertures. In the center of the domain, a solid wall of thickness $h = 1$ mm presents a circular orifice of diameter $2a = 1$ mm. The porosity of the plate is then given by $\sigma = \pi a^2 / d^2 = 2.18\%$. To avoid unsuitable interactions between the boundary conditions and the flow around the orifice, the inlet and outlet boundaries are located at a large distance $L = 120a$ from the aperture. Non-reflecting acoustic conditions are imposed at both inlet and outlet boundaries. The computational mesh contains 643000 tetrahedra, and the orifice diameter $2a$ has been discretized with at least 20 points in the radial direction. Figure 2 shows an enlargement of the mesh near the orifice.

In all the simulations conducted in this study, a mean bias flow passes through the aperture (from left to right in Fig. 1). The application envisaged for the configuration analyzed in this work is the use of perforated plates backed by a resonant cavity to damp low frequency combustion instabilities at the inlet of an injection system, as studied by Tran *et al.* [3]. This type of low frequency thermo-acoustic interactions features typically self-sustained oscillations of a few hundred Hertz. It was chosen to conduct the analysis here for a modulation frequency $f = 400$ Hz. For the application considered here, incident acoustic waves are normal to the plate and the temperature of the gases remains cool.

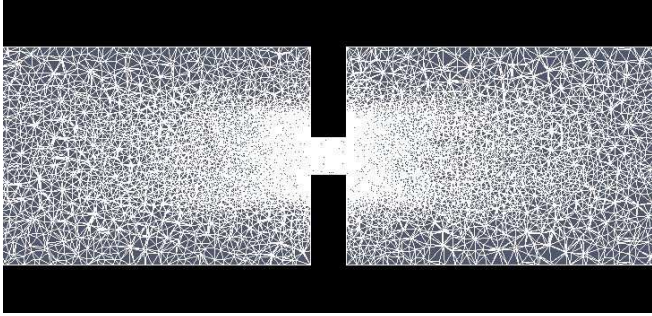


FIGURE 2: LONGITUDINAL CUT OF THE THREE-DIMENSIONAL COMPUTATIONAL MESH NEAR THE ORIFICE.

The case considered is an isothermal flow of nitrogen characterized by a density $\rho = 1.18 \text{ kg m}^{-3}$ with a temperature $T_\infty = 300 \text{ K}$. Nitrogen is injected at the inlet with a small uniform velocity $\bar{u} = 0.074 \text{ m s}^{-1}$. This flow velocity corresponds to a bulk velocity in the aperture is $\bar{u}_0 = \bar{u}/\sigma = 3.4 \text{ m s}^{-1}$. At this operating point, the Mach number in the orifice is $M_0 = \bar{u}_0/c \simeq 0.01$ and the Reynolds number $\text{Re}_0 = \bar{u}_0 2a/\nu \simeq 220$.

The mean pressure imposed at the outlet is $p_a = 101300 \text{ Pa}$. The acoustic forcing is obtained by adding a harmonic oscillation to the characteristic pressure wave entering the domain (I in Fig. 1), with a constant frequency $f = 400 \text{ Hz}$. These forcing conditions correspond to a Strouhal number $\text{St} = \omega a/\bar{u}_0 = 0.37$, which approaches optimal acoustic absorption $\alpha = 0.42$ for small perturbation levels [8]. The amplitude of the incoming acoustic wave is then varied from 0.89 to 890 Pa. This corresponds to sound pressure levels (SPL) ranging from 90 dB up to 150 dB. Nine different simulations were conducted to investigate both the linear (low forcing amplitude) and nonlinear regimes (high forcing amplitude). These calculations are run over 40 modulation periods and only the last 20 periods were post-processed to examine the acoustic properties. The hypothesis of plane wave propagation away from the orifice has been verified in the computations. The maximum phase difference between two pressure signals taken at different points in the same cross-section at $l/2a = 50$ away from the orifice is less than 1 degree, and the maximum amplitude difference reaches 0.3%. At the forcing frequency $f = 400 \text{ Hz}$ considered here, the ratio between the orifice diameter $2a$ and the acoustic wavelength λ is small enough $2a/\lambda = 1.2 \times 10^{-3} \ll 1$, so that the interaction can be considered compact. No higher modes were observed, except the harmonics of the modulation frequency at high SPL. Far from the orifice, the amplitude of the second harmonic of the modulation frequency observed in the pressure spectrum is lower by at least one order of magnitude than the amplitude of the fundamental peak.

RESULTS

Flow visualization

Figures 3 and 4 show the vorticity field in the vicinity of the perforation during a forcing cycle at 400 Hz for two different forcing amplitudes. Note that in these figures, only a fraction of the numerical domain is represented upstream and downstream the orifice over a distance $l/2a = 20$. The numerical domain extends up to $l/2a = 60$. In these images, the mean flow is oriented from the bottom to the top. Flow separation appears at the edges of the aperture, due to the effect of viscosity. In Fig. 3 a moderate perturbation level is applied at the outlet of the domain, corresponding to an incident sound level SPL = 110 dB at this location. The acoustic perturbation incident on the jet generates a convective modulation of the vorticity field in the direction of the flow synchronized by the forcing frequency. These fluctuations are only visible on the jet flowing through the aperture downstream the perforation. The vorticity field below the plate is not affected by these perturbations during the modulation cycle and remains constant. The flow remains axisymmetric during the forcing cycle. The vorticity wave is swept away by the mean flow above the plate and is then dissipated by turbulence at large distance from the orifice. By following the position of the maximal vorticity magnitude z_{vort} in the jet at the different phases in the cycle, one finds that these vorticity disturbances triggered by the acoustic waves are convected at a velocity approaching that of the mean flow $\Delta z_{\text{vort}}/\Delta t \simeq \bar{u}_0$. This behavior is in agreement with the classical scenario [4, 8], but the situation is different for a higher modulation level.

At high forcing amplitude, the structure of the unsteady flow changes significantly. Figure 4 shows the vorticity field for an incident SPL of 140 dB. The vorticity field now features large fluctuations on both sides of the perforation with a change of sign during the modulation cycle. The flow within the perforation is pulling large vortex rings which are alternatively convected downstream and upstream the plate. These large coherent structures go deeper within the flow, at a larger distance from the perforation, before being dissipated by turbulence and viscous processes. The convection speed of the vortices before reverse flow occurs now scales with the fluctuating velocity in the orifice $\Delta z_{\text{vort}}/\Delta t \simeq u'_0$ ($t/T_p \leq 0.50$). The unsteady flow remains axisymmetric only in the vicinity of the orifice. These changes in the flow deeply impact the acoustic properties of the aperture, as shown below.

Sound level effects

It is interesting to compare the values of the reflection and transmission coefficients computed from the results of the numerical simulations with the predictions of the linear model Eq. (5) when the modulation level is increased. The reflection

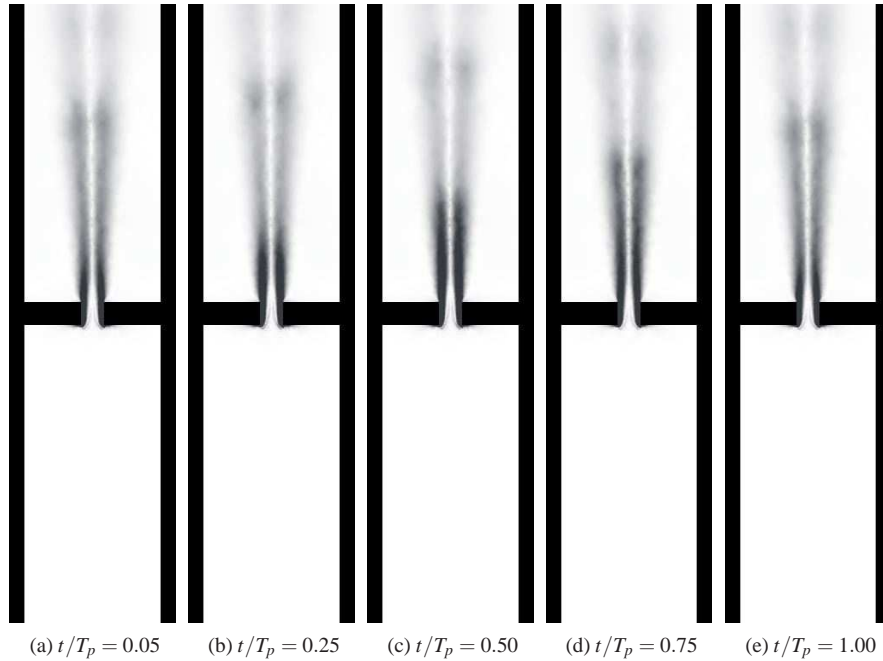


FIGURE 3: INSTANTANEOUS VORTICITY FIELD AT 110 dB, DURING A FORCING CYCLE AT 400 Hz. VORTICITY MAGNITUDE FROM 0 (WHITE) TO $1.5\bar{u}_0/a$ (BLACK).

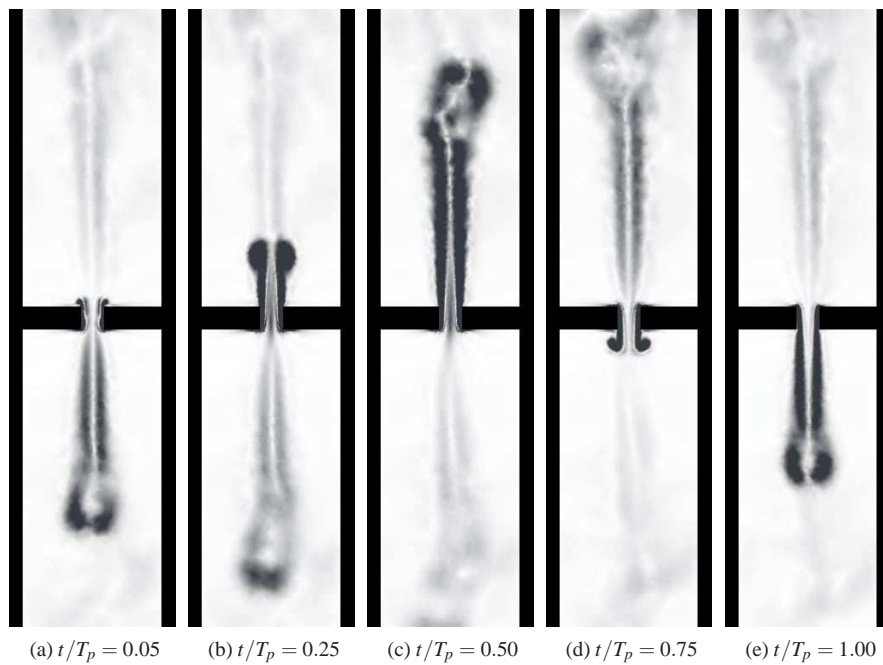


FIGURE 4: INSTANTANEOUS VORTICITY FIELD AT 140 dB, DURING A FORCING CYCLE AT 400 Hz. VORTICITY MAGNITUDE FROM 0 (WHITE) TO $3.5\bar{u}_0/a$ (BLACK). NOTE THAT THE SCALING FACTOR IS NOT THE SAME AS IN FIG. 3.

coefficient R is determined in the simulations as follows (Fig. 1):

$$R = \frac{\zeta + 1}{\zeta - 1}, \quad (7)$$

where $\zeta = \tilde{p}_d / \rho c \tilde{u}_d$ is the specific impedance of the orifice. The pressure fluctuation \tilde{p}_d and the corresponding longitudinal velocity disturbance \tilde{u}_d are taken here at a distance $l/2a = 50$ downstream the orifice, in a region where the flow is uniform away from the jet. In nonlinear regimes, \tilde{p} and \tilde{u} represent the fundamental-harmonic components of pressure and velocity fluctuations, respectively. Knowing the reflection coefficient and the pressure fluctuation \tilde{p}_u at a distance $l/2a = 50$ upstream the orifice, it is also possible to compute the modulus of the transmission coefficient of the orifice:

$$|T| = \left| \frac{\tilde{p}_u}{\tilde{p}_d} (1 + R) \right| \quad (8)$$

Figure 5 shows the modulus of reflection and transmission coefficients extracted from the simulations and compared to the predictions from Eq. (5). As expected, the agreement is good at low to moderate excitation levels ($\text{SPL} \leq 120$ dB), thus validating the methodology. For sound levels larger than 130 dB, $|R|$ and $|T|$ depend on the acoustic perturbation amplitude. The reflected wave amplitude grows, whereas the amplitude of the transmitted wave drops when the sound level increases.

It is difficult to further analyze the results by only considering the acoustic properties far from the orifice. A quantity more relevant to the flow dynamics in the vicinity of the perforation is the ratio between the fluctuating velocity u'_0 averaged over the cross section of the orifice and the bulk velocity \bar{u}_0 within the orifice. Figure 6 shows the temporal evolution of the ratio u'_0/\bar{u}_0 for three different SPL, over an oscillation period. The lines $u'_0 = -\bar{u}_0$ and $u'_0 = \bar{u}_0$ are also plotted. When the temporal signal crosses the $u'_0 = -\bar{u}_0$ line, reverse flow appears in the orifice during the forcing cycle. For sound levels lower than $\text{SPL} \leq 120$ dB, no reverse flow occurs. This is not the case for higher sound levels. When the SPL is higher than 130 dB, the velocity fluctuation amplitude becomes higher than the mean bias flow velocity, and then reverse flow is observed during part of the excitation cycle. Vortex rings are then released alternatively from both sides of the aperture, as indicated in Fig. 4, thus changing the way acoustic waves are dissipated.

Analysis of absorption

Figure 7 plots the evolution of the absorption coefficient versus \tilde{u}_0/\bar{u}_0 in the orifice for the different cases explored. The simulations match well with the predictions of the modulus of the reflection coefficient $|R|$ for perturbation levels lower than

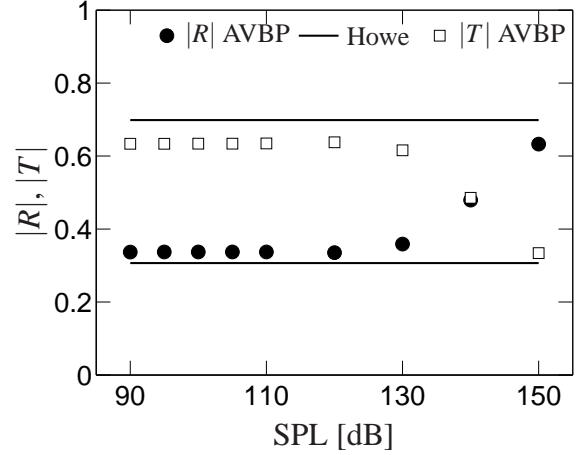


FIGURE 5: REFLECTION AND TRANSMISSION COEFFICIENTS VERSUS SPL, AT 400 Hz. COMPARISON BETWEEN LES RESULTS AND HOWE'S LINEAR MODEL.

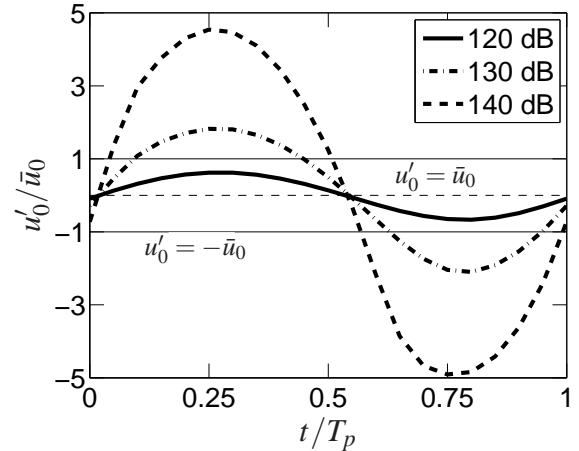


FIGURE 6: EVOLUTION OF THE RELATIVE VELOCITY FLUCTUATION RATIO IN THE ORIFICE u'_0/\bar{u}_0 , DURING A FORCING CYCLE AT 400 Hz, FOR DIFFERENT SPL.

120 dB. A slight difference is observed in the modulus of the transmission coefficient T but surprisingly, there is a relatively fairly good agreement between theoretical predictions and the LES results even at high amplitudes. It is shown that absorption remains roughly constant over the whole range of perturbation levels explored, covering several orders of magnitude \tilde{u}_0/\bar{u}_0 varying from 0.02 to 10.

However, the way the incident acoustic energy is dissipated differs at low and high amplitudes. In Fig. 7 the contributions of the reflected and the transmitted waves to absorption are also

indicated. As long as the velocity fluctuation within the orifice \tilde{u}_0 remains smaller than the mean bias flow velocity \bar{u}_0 , the reflection and transmission coefficients remain independent of the sound level. In this case sound absorption within this orifice at a forcing frequency of 400 Hz nearly reaches the maximal theoretical value $\alpha_{\max} = 0.5$, and is mainly due to the low amplitude of the reflected wave. When the velocity fluctuation \tilde{u}_0 exceeds the mean bias flow velocity, the modulus of the reflection coefficient begins to increase with increasing amplitude and its contribution to absorption drops correspondingly. This loss is however balanced by the increasing contribution of the transmitted wave, because its modulus $|T|$ decreases with the forcing amplitude. Globally, the energy transfer process taking place between the acoustic field and the unsteady flow leads to approximately the same fraction of acoustic energy dissipated for velocity perturbation levels covering two decades, when $\tilde{u}_0 \ll \bar{u}_0$ as well as when $\tilde{u}_0 \gg \bar{u}_0$ (at least for $\tilde{u}_0/\bar{u}_0 \leq 10$). This suggests that a unified model based on energy considerations should be able to describe the orifice response in these different regimes $\tilde{u}_0/\bar{u}_0 \ll 1$ (linear) and $\tilde{u}_0/\bar{u}_0 \gg 1$ (nonlinear) for input levels lower than $\tilde{u}_0/\bar{u}_0 \leq 10$.

Acoustic energy is mainly dissipated here by vorticity. At small disturbance levels, vorticity is only produced downstream with the formation of vortex rings. When acoustic velocities within the orifice are smaller than the mean bias flow velocity, vorticity production is dominated by the mean flow (see Fig. 3). Values of the reflection, transmission and absorption coefficients are then found constant at small disturbance levels. For acoustic velocities larger than the mean bias flow velocity, reverse flow appears and vortex rings are swept away from both sides of the orifice (see Fig. 4). Dissipation takes place in this case both upstream and downstream the orifice, and this process is mainly governed by the amplitude of the fluctuating flow in the orifice.

The temporal pressure signals plotted in Figs. 8 and 9 confirm this analysis. For a small modulation corresponding to 110 dB (Fig. 8), the velocity fluctuation amplitude in the orifice reaches 20 % of the mean bias flow velocity and reverse flow is absent. The ratio between the amplitude of the transmitted pressure wave at the inlet of the domain and the pressure fluctuation at the outlet is approximately equal to 1/2. At 150 dB (Fig. 9) this ratio is reduced to approximately 1/6. It is three times smaller than in 110 dB case, whereas the velocity fluctuation in the orifice is 10 times larger than the mean bias flow velocity. The transmission coefficient is thus much smaller at 150 dB, as shown in Fig. 5. In this case, the time traces of the transmitted pressure and the velocity fluctuations in the orifice, averaged over the cross section, are not pure harmonic signals at high amplitude. This indicates a nonlinear response of the aperture. For a forcing level at 150 dB, the velocity fluctuation within the perforation reaches $\tilde{u}_0/\bar{u}_0 = 10$. The nonlinearity observed on the sound waves at large distance from the orifice in Fig. 9 remains however weak and can probably be treated by a weakly

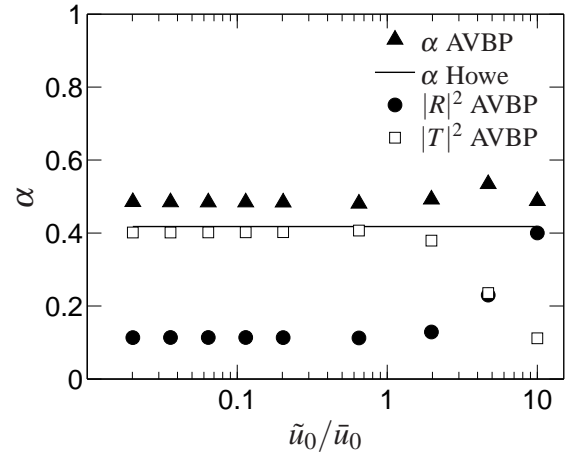


FIGURE 7: ABSORPTION COEFFICIENTS VERSUS \tilde{u}_0/\bar{u}_0 , AT 400 HZ. COMPARISON BETWEEN LES RESULTS AND HOWE'S LINEAR MODEL.

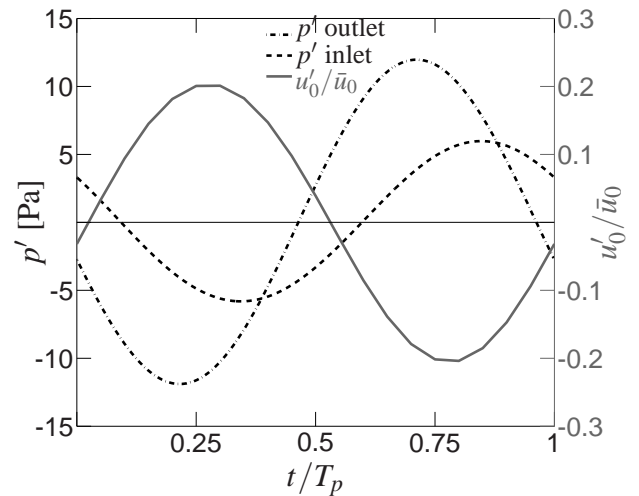


FIGURE 8: TEMPORAL PRESSURE SIGNALS AT THE DOMAIN INLET AND OUTLET, AND INSTANTANEOUS VELOCITY RATIO IN THE ORIFICE u'_0/\bar{u}_0 , EXTRACTED FROM NUMERICAL SIMULATION. EXCITATION AT 400 HZ AND 110 dB.

nonlinear analysis.

Different types of analysis were envisaged to treat the non-linearity of the orifice response. Many of them consider the unsteady pressure loss through the orifice caused by the acoustic modulation under quasi-steady assumption [27, 28]. This pres-

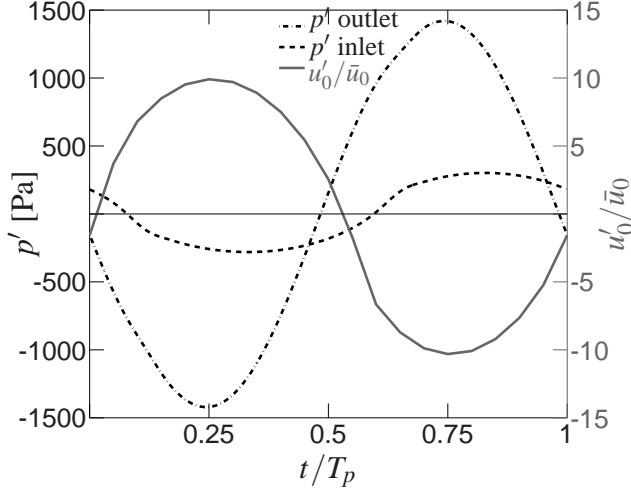


FIGURE 9: TEMPORAL PRESSURE SIGNALS AT THE DOMAIN INLET AND OUTLET, AND INSTANTANEOUS VELOCITY RATIO IN THE ORIFICE u'_0/\bar{u}_0 , EXTRACTED FROM NUMERICAL SIMULATION. EXCITATION AT 400 Hz AND 150 dB.

sure loss writes [19]:

$$\Delta p = \frac{1}{2} \rho \eta |u_0| u_0, \quad (9)$$

where η is the pressure loss coefficient and u_0 the bias flow velocity in the orifice. The absolute value in this expression takes into account a possible reverse flow in the orifice. When this velocity is modulated $u_0 = \bar{u}_0 + u'_0$, it is possible to write Eq. (9) in terms of the fluctuating pressure loss:

$$\Delta p' = \frac{1}{2} \rho \bar{u}_0^2 \eta \left[1 + \frac{u'_0}{\bar{u}_0} \left(1 + \frac{u'_0}{\bar{u}_0} \right) - 1 \right] \quad (10)$$

This expression was used by Bellucci *et al.* [20] to analyze the response of perforates in both linear and nonlinear absorption regimes. Equation (10) was treated in the frequency domain.

The problem is then to specify the pressure loss coefficient η . In the linear absorption regime $\bar{u}_0 \ll \bar{u}_0$, the model developed by Howe [4] can be used. By combining the linearized form of Eq. (10) and Eq. (2) for the Rayleigh conductivity with Eq. (3), the pressure loss coefficient can be written as a function of the Strouhal number only:

$$\eta = \frac{\pi St}{2} \frac{\delta}{\gamma^2 + \delta^2} \quad (11)$$

At very high acoustic levels, the fluctuating velocity in the orifice is significantly larger than the mean bias flow velocity $\bar{u}_0 \gg \bar{u}_0$. This justifies the use of a nonlinear model based on a *vena contracta* approach [15, 18, 20, 27]. The pressure loss coefficient is then approximated by a constant discharge coefficient C_D :

$$\eta = \frac{1}{C_D^2} \quad (12)$$

Bellucci *et al.* [20] used in their analysis a heuristic expression (Eq. (32) in that reference) to examine the values taken by the pressure loss coefficient η during the transition between the linear and nonlinear regimes. It is assumed in that study that the linear expression Eq. (10) is valid for velocity fluctuations lower than \bar{u}_0 and that the pressure loss coefficient tends toward Eq. (12) at very high sound levels. Predictions with this model for the evolution of the pressure loss coefficient as a function of the disturbance level are reproduced in Fig. 10 as dashed lines. The value used for the discharge coefficient $C_D = 0.82$ in this figure is the same as the one used by these authors for a single orifice without mean bias flow.

It is possible to compare these predictions with results extracted from LES simulations. A Fast Fourier Transform (FFT) algorithm is applied to the fluctuating pressure signals recorded at large distance from the orifice in the simulations. This enables to determine the pressure difference fluctuation amplitude $\Delta \bar{p}$ examined at the forcing frequency $f = 400$ Hz. The same procedure is applied to the right-hand side term in Eq. (10). The velocity signal is first averaged over the orifice cross section and the right-hand side term in Eq. (10) is calculated in the time domain. The first harmonic component of this signal is then calculated with the FFT algorithm. This is used to examine the evolution of the pressure loss coefficient η at the forcing frequency as a function of the velocity ratio \bar{u}_0/\bar{u}_0 in the orifice.

These numerical estimates are compared in Fig. 10 to the predictions of the three models presented above. At low to moderate modulation levels, the simulations show good agreement with the linear model Eq. (11), while the constant value taken by η is slightly underpredicted by this model compared to numerical results. The pressure loss coefficient takes a constant value up to a velocity ratio $\bar{u}_0/\bar{u}_0 = 2$ in the simulations while Bellucci *et al.* fix the transition to nonlinearity at $\bar{u}_0/\bar{u}_0 = 1$. For $\bar{u}_0/\bar{u}_0 > 2$, numerical estimates of η decrease with the velocity fluctuation level, approaching the value $\eta = 1.49$ predicted by the nonlinear model Eq. (12) for $C_D = 0.82$. This limit value is reached for $\bar{u}_0/\bar{u}_0 \geq 6$ in the heuristic approach of Bellucci *et al.* For $\bar{u}_0/\bar{u}_0 \simeq 10$ simulations yield $\eta \simeq 1.65$. While the correct limits at small and high oscillation amplitudes are predicted, the transition level between linear to nonlinear regimes and the saturation at higher oscillation levels are not properly reproduced by the heuristic approach. It should however be noted that the

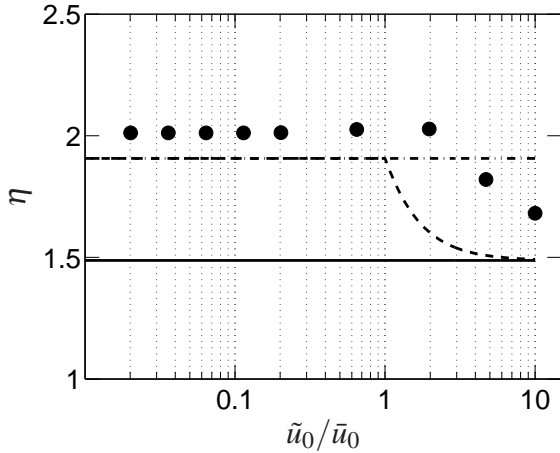


FIGURE 10: PRESSURE LOSS COEFFICIENT η VERSUS \tilde{u}_0/\bar{u}_0 , AT 400 Hz. COMPARISON BETWEEN LES RESULTS (\bullet) AND ANALYTICAL MODELS: LINEAR MODEL FROM EQ. (11) (DASH-DOTTED LINE), NONLINEAR MODEL FROM EQ. (12) (SOLID LINE) AND BELLUCCI ET AL. HEURISTIC TRANSITION MODEL (DASHED LINE).

saturation level found at high oscillation amplitudes depends on the value chosen for C_D . The numerical value used here and in Ref. [20] $C_D = 0.82$ is not the only possible choice. The discharge coefficient C_D was thus computed for the steady flow in absence of external disturbances, and post-processing of the LES data yielded a value $C_D = 0.62$. This numerical estimate is consistent with classical values found for a steady jet through a small orifice [18, 29]. One can however see that the saturation level reached by the pressure drop coefficient $\eta = 2.58$ calculated with this value for the discharge coefficient $C_D = 0.62$ is much higher than the one reached in the simulations. This indicates that it is probably difficult to deduce the correct saturation value of the pressure loss coefficient from steady simulations and motivates further analysis of sound absorption mechanisms at high amplitude. Results must also be gathered at other forcing frequencies and further numerical simulations must be conducted.

CONCLUSION

Three-dimensional large eddy simulations of the flow through an orifice submitted to low frequency sound waves of increasing levels have been carried out. The analysis conducted here has shown that the knowledge of the induced velocity fluctuation amplitude in the aperture is crucial to properly analyze the acoustic response of an orifice traversed by a bias flow. The transition between the linear regime, where acoustic properties are independent of the sound level, and nonlinear regime, where these properties strongly depend on the perturbation amplitude,

takes place when the fluctuating acoustic velocity in the orifice becomes larger than the bulk velocity. When this limit value is exceeded, reverse flow appears, and vortex rings are shed on both sides of the orifice. The absorption coefficient of the orifice remains however almost constant over the amplitude range simulated here, covering $\tilde{u}_0/\bar{u}_0 = 0.02$ to 10, but both the reflection and transmission coefficients of sound waves are strongly modified at high modulation amplitudes. When the incident wave amplitude is increased, acoustic energy dissipation decreases at the reflection side and increases at the transmission side of the aperture. Comparisons between numerical estimates of the unsteady pressure loss through the orifice with different analytical models show that the general trends and the limits are well retrieved, but work is still required to capture the correct transition level between the linear and nonlinear regimes and to predict the correct saturation at higher levels. These results help in understanding the behavior of perforated plates at high sound levels, and motivate the seek of a unified model in linear and nonlinear regimes based on energy considerations.

ACKNOWLEDGEMENT

This work is supported by the Direction Générale de l'Armement (DGA) in the form of a PhD fellowship. The authors are grateful to the CINES (Centre Informatique National pour l'Enseignement Supérieur) and GENCI (Grand Équipement National de Calcul Intensif) for the access to supercomputer facilities.

REFERENCES

- [1] Candel, S., 2002. "Combustion dynamics and control: Progress and challenges". *Proceedings of the Combustion Institute*, **29**(1), pp. 1–28.
- [2] Lieuwen, T., and Yang, V., 2005. "Combustion instabilities in gas turbine engines, operational experience, fundamental mechanisms and modeling". *Progress in Astronautics and Aeronautics AIAA*, **210**.
- [3] Tran, N., Ducruix, S., and Schuller, T., 2009. "Damping combustion instabilities with perforates at the premixer inlet of a swirled burner". *Proceedings of the Combustion Institute*, **32**(2), pp. 2917–2924.
- [4] Howe, M. S., 1979. "On the theory of unsteady high reynolds number flow through a circular aperture". *Proceeding of the Royal Society*, **366**, pp. 205–223.
- [5] Hughes, I. J., and Dowling, A. P., 1990. "The absorption of sound by perforated linings". *Journal of Fluid Mechanics*, **218**, pp. 299–335.
- [6] Tran, N., Ducruix, S., and Schuller, T., 2009. "Passive control of the inlet acoustic boundary of a swirled burner at high amplitude combustion instabilities". *Journal of*

- Engineering for Gas Turbines and Power*, **131**(5), 09, pp. 051502–7.
- [7] Melling, T. H., 1973. “The acoustic impedance of perforates at medium and high sound pressure levels”. *Journal of Sound and Vibration*, **29**(1), 7, pp. 1–65.
- [8] Howe, M. S., 1998. *Acoustics of fluid-structure interactions*. Cambridge University Press, Cambridge.
- [9] Wendoloski, J. C., 1998. “Sound absorption by an orifice plate in a flow duct”. *The Journal of the Acoustical Society of America*, **104**(1), 07, pp. 122–132.
- [10] Jing, X., and Sun, X., 2000. “Effect of plate thickness on impedance of perforated plates with bias flow”. *AIAA Journal*, **38**(9), pp. 1573–1578.
- [11] Dupère, I. D. J., and Dowling, A. P., 2001. “The absorption of sound near abrupt axisymmetric area expansions”. *Journal of Sound and Vibration*, **239**, pp. 709–730.
- [12] Lee, F. C., and Chen, W. H., 2003. “On the acoustic absorption of multi-layer absorbers with different inner structures”. *Journal of Sound and Vibration*, **259**(4), 1, pp. 761–777.
- [13] Lee, S.-H., Ih, J.-G., and Peat, K. S., 2007. “A model of acoustic impedance of perforated plates with bias flow considering the interaction effect”. *Journal of Sound and Vibration*, **303**(3-5), 6, pp. 741–752.
- [14] Rupp, J., Carrotte, J., and Spencer, A., 2010. “Interaction between the acoustic pressure fluctuations and the unsteady flow field through circular holes”. *Journal of Engineering for Gas Turbines and Power*, **132**(6), 06, pp. 061501–9.
- [15] Ingard, U., and Ising, H., 1967. “Acoustic nonlinearity of an orifice”. *The Journal of the Acoustical Society of America*, **41**(6), 01, pp. 1582–1583.
- [16] Leung, R. C. K., So, R. M. C., Wang, M. H., and Li, X. M., 2007. “In-duct orifice and its effect on sound absorption”. *Journal of Sound and Vibration*, **299**(4-5), 2, pp. 990–1004.
- [17] Mendez, S., and Eldredge, J. D., 2009. “Acoustic modeling of perforated plates with bias flow for large-eddy simulations”. *Journal of Computational Physics*, **228**(13), 7, pp. 4757–4772.
- [18] Cummings, A., and Eversman, W., 1983. “High amplitude acoustic transmission through duct terminations: Theory”. *Journal of Sound and Vibration*, **91**(4), 12, pp. 503–518.
- [19] Cummings, A., 1986. “Transient and multiple frequency sound transmission through perforated plates at high amplitude”. *The Journal of the Acoustical Society of America*, **79**(4), 04, pp. 942–951.
- [20] Bellucci, V., Flohr, P., and Paschereit, C., 2004. “Numerical and experimental study of acoustic damping generated by perforated screens”. *AIAA Journal*, **42**(8), pp. 1543–1549.
- [21] Hofmans, G. C. J., Boot, R. J. J., Durrieu, P. P. J. M., Auregan, Y., and Hirschberg, A., 2001. “Aeroacoustic response of a slit-shaped diaphragm in a pipe at low helmholtz number, 1: quasi-steady results”. *Journal of Sound and Vibration*, **244**(1), 6, pp. 35–56.
- [22] Luong, T., Howe, M. S., and McGowan, R. S., 2005. “On the rayleigh conductivity of a bias-flow aperture”. *Journal of Fluids and Structures*, **21**(8), 12, pp. 769–778.
- [23] Dowling, A. P., and Hughes, I. J., 1992. “Sound absorption by a screen with a regular array of slits”. *Journal of Sound and Vibration*, **156**(3), 8, pp. 387–405.
- [24] Schönfeld, T., and Rudgyard, M., 1999. “Steady and unsteady flows simulations using the hybrid flow solver avbp”. *AIAA Journal*, **37**(11), pp. 1378–1385.
- [25] Nicoud, F., and Ducros, F., 1999. “Subgrid-scale stress modelling based on the square of the velocity gradient tensor”. *Flow, Turbulence and Combustion*, **62**, pp. 183–200.
- [26] Poinso, T., and Lele, S. K., 1992. “Boundary conditions for direct simulations of compressible viscous flows”. *Journal of Computational Physics*, **101**(1), 7, pp. 104–129.
- [27] Peters, M. C. A. M., Hirschberg, A., Reijnen, A. J., and Wijnands, A. P. J., 1993. “Damping and reflection coefficient measurements for an open pipe at low mach and low helmholtz numbers”. *Journal of Fluid Mechanics*, **256**, pp. 499–534.
- [28] Durrieu, P., Hofmans, G., Ajello, G., Boot, R., Auregan, Y., Hirschberg, A., and Peters, M. C. A. M., 2001. “Quasi-steady aero-acoustic response of orifices”. *Journal of the acoustical society of America*, **110**(4), pp. 1859–1872.
- [29] Batchelor, G. K., 1967. *An Introduction to Fluid Dynamics*. Cambridge University Press, Cambridge.